



Cite this: *Chem. Commun.*, 2023, 59, 3431

Received 27th January 2023,
Accepted 20th February 2023

DOI: 10.1039/d3cc00384a

rsc.li/chemcomm

The tailored design of a light-triggered supramolecular cascade results in an artificial machinery that assimilates the transduction of photons into chemical communication and the final release of a neurotransmitter. This is reminiscent of key steps in the natural vision process.

The vision process is an intricate and complex example of chemical signal cascading, triggered by light as an external stimulus. In a nutshell, photons are used by 11-cis retinal, resulting in its conversion into all-trans retinal.¹ This transformation is accompanied by structural changes of rhodopsin, which subsequently triggers a series of concatenated chemical signaling events. Ultimately this leads to a depletion of cGMP and the closing down of Na^+ ion channels, which results in an attenuation of the dark current and the hyperpolarization of the photoreceptor cells.² The retina is further composed of other cells that are intercommunicated in a circuit, thereby enabling the gift of vision in all its facets: three-dimensional vision, color perception, adaption to light intensity conditions, *etc.* Among these cellular components are amacrine cells,² a diverse group of interneurons in the retina, which are responsible for the modulation between bipolar and ganglion cells.

Dopamine is essential for the regulation of light-adapted vision and photoreceptor coupling in the retina. This neurotransmitter is released by dopaminergic amacrine cells, following a light-intensity-modulated circadian rhythm (see Fig. 1).³ Within this context we sought to realize an artificial light-driven host-guest system^{4,5} that would mimic the following features:

^a CIQSO – Centre for Research in Sustainable Chemistry and Department of Chemistry, University of Huelva, Campus de El Carmen s/n, E-21071, Huelva, Spain.

E-mail: uwe.pischel@diq.uhu.es; Tel: +34 959 21 99 82

^b Laboratorio Associado para a Química Verde (LAQV), Rede de Química e Tecnologia (REQUIMTE), Departamento de Química, Faculdade de Ciências e Tecnologia, Universidade NOVA de Lisboa, 2829-516, Caparica, Portugal

† Electronic supplementary information (ESI) available: General methods and materials, additional NMR data for the individual competitive displacement events, NMR titrations of both forms of 1 with CB7, and formalism for speciation simulation. See DOI: <https://doi.org/10.1039/d3cc00384a>

Phototransduction in a supramolecular cascade: a mimic for essential features of the vision process†

Jialei Chen-Wu,^a Patrícia Máximo,^{id}^b Patricia Remón,^{id}^a A. Jorge Parola,^{id}^b Nuno Basílio^{id}^b and Uwe Pischel^{id}^a

light-induced structural changes that lead to a cascade of supramolecular events,^{6–16} culminating in the final release of dopamine.

We decided to design our system based on the host-guest chemistry of cucurbit[n]urils (CBn).^{17–19} These water-soluble macrocycles feature a hydrophobic inner cavity with low polarizability and carbonyl-rimmed portals. Hence, guests that can exert hydrophobic effects and ion-dipole interactions lead to the formation of highly stable complexes, which often reach affinities in the subnanomolar range.^{17,19,20} Depending on the size and shape of the guest and the resulting packing in the complex, a highly selective binding to different CBn homologues ($n = 7$ and 8 in our case) can be observed. This may lead to affinity differentiations of up to 5–7 orders of magnitude. Taking advantage of the high-affinity binding, CBn has been applied in bio-relevant applications,^{21,22} drug delivery,²³ functional materials,²⁴ and sensing,^{25–28} among others.

Light as an external stimulus of supramolecular assemblies is very attractive due to the possibility of spatiotemporal control.^{29–39} This has been explored as well in the context of CBn chemistry.^{40–43} Among other photoswitches, dithienylethenes (DTEs)^{44–46} have been proven very useful^{47–51} and will also play a crucial role in the present work.

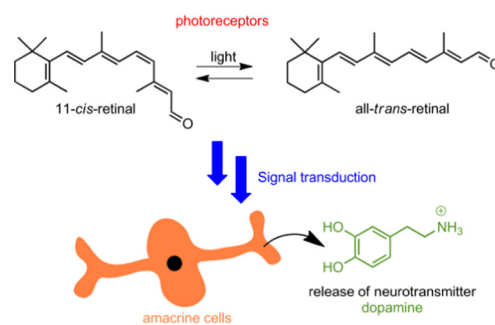


Fig. 1 Representation of the photoisomerization of 11-cis-retinal and signal transduction, triggering dopamine release from amacrine cells.



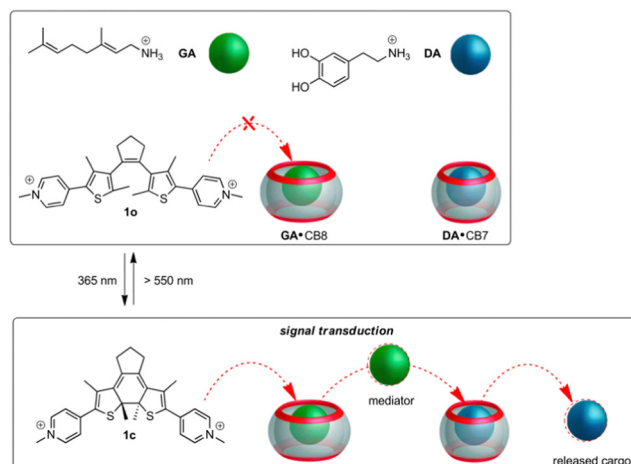


Fig. 2 Design of the light-controlled supramolecular cascade in a self-sorted five-component mixture.

The design approach towards the envisioned light-controlled supramolecular cascade is outlined in Fig. 2. The initial state of the five-component mixture is expected to obey the rules of thermodynamically controlled self-sorting. The DTE photoswitch in its non-activated form (**1o**) should not occupy any of the host macrocycles, while the mediator guest is bound by CB8 and dopamine (**DA**) is allocated inside the CB7 cavity. On photoactivation of the switch a competitor is formed (**1c**) that displaces the mediator from CB8, which then competes with **DA** for the CB7 macrocycle. This would result in the effective release of the neurotransmitter. Importantly, the activated photoswitch should not bypass the mediator function and displace dopamine directly from CB7.

As can be expected for such an intricate situation, a judicious choice of the guests is indispensable (see Table 1). The mediator should bind much stronger to CB8 than to CB7, but still have a CB7-affinity that at least equals that of **DA** ($K_{DA-CB7} = 1.1 \times 10^5 \text{ M}^{-1}$).¹⁶ We identified geranylamine (**GA**) to fit this bill conveniently, being a subnanomolar-affinity binder for CB8 and a micromolar-affinity binder for CB7 ($K_{GA-CB8}/K_{GA-CB7} \text{ ca. } 5000$);^{49,52} see Table 1. The DTE photoswitch should show a large CB8-affinity differentiation for its activated and non-activated forms,⁵¹ while being a poor binder for CB7 in any of its forms. To our satisfaction, switch **1** in both forms (**1o** and

1c) shows very low binding (*ca.* 10^3 M^{-1}) with CB7; see Table 1. However, for CB8 high-affinity binding at the subnanomolar level is observed for **1c**, while **1o** binds *ca.* 4000 times less strong.⁵¹ The absolute CB8-binding affinity of **1c** is even somewhat higher than that of **GA**; see Table 1. Based on these data a light-induced cascade should be feasible.

In the following steps, we sought to obtain experimental confirmation for this premise. ^1H NMR spectroscopy is the method of choice to follow the distinct situations of the guests being unbound or complexed by one of the two CB homologues. When mixing equimolar amounts (200 μM each in D_2O at $\text{pD } 5.4$) of guests **GA** and **DA** and the hosts CB7 and CB8 a clear-cut self-sorting situation is encountered (see ESI†). As predicted from the guest affinities for each host (see Table 1), **GA** is complexed exclusively by CB8, while **DA** is bound by CB7. This is for example indicated by typical upfield shifts of the methyl protons of **GA**.⁴⁹ Noteworthily, the ^1H NMR signature of **GA** when complexed by CB7 or CB8 is well differentiated and can be unambiguously assigned to the latter situation (see the spectra in ESI†). The proton signals of **DA** broaden to such an extent that they are not visible in the CB7 complex.¹⁶ The next question that arises is whether **GA** can displace **DA** from its CB7 complex. When adding 200 μM **GA** to the **DA-CB7** complex (also at 200 μM) the appearance of free **DA**, signalled by the typical aromatic proton signals at 6.8–6.9 ppm, is detected (see ESI†). Also the characteristic signature of the **GA-CB7** complex appears. However, some **GA** (about 50%) remains non-complexed. In the following we evaluated whether the DTE in either form (**1o** or **1c**) would displace **GA** from its CB8 complex. For this, a solution (D_2O , $\text{pD } 5.4$) with 300 μM **1o** and 200 μM **GA-CB8** was prepared. Gratifyingly **1o** does not displace **GA**. This is expected, due to the four orders of magnitude smaller binding constant of **1o** with the macrocycle (see Table 1). However, when isomerising **1o** into **1c** by irradiation with 365 nm light ($\Phi_{1o \rightarrow 1c} = 0.04$; quantitative conversion),⁵¹ competition is observed which results in an efficient release of **GA** from the CB8 macrocycle (*ca.* 90%); see the ESI.†

Having gathered compelling experimental proof for the stepwise competitive displacement of **GA** from CB8 (by means of the action of photogenerated **1c**) and **DA** from CB7 (by means of the action of **GA**), we proceeded to the complete cascade experiment in the five-component mixture ($[1o] = 300 \mu\text{M}$, $[DA] = [GA] = [CB7] = [CB8] = 200 \mu\text{M}$). As anticipated, in this system a very clear self-sorting applies: **GA** is encountered in CB8, **DA** in CB7, and **1o** is not complexed by any of the macrocycles (see Fig. 3a). In agreement, only the proton signals of **GA** in CB8 are observed. The aromatic signals of **DA** are not visible at all, as expected due to its complexation by CB7. The DTE signals correspond to non-complexed open form **1o**, indicating that this form of the switch does not occupy the CB8 cavity. On photoisomerization (365 nm light), forming **1c**, **GA** is found in CB7 (about 90% of the **GA** is competitively displaced from CB8 by **1c**), **1c** in CB8 (beside some amount of free **1c**, due to the excess concentration of the photoswitch) and the aromatic ^1H NMR signals of released **DA** are clearly seen (see Fig. 3b). By comparison of the integrated ^1H NMR signals

Table 1 Binding constants of DTE **1**, geranylamine (**GA**), and dopamine (**DA**) with CB7 and CB8

Complex	K/M^{-1}
DA-CB7^a	1.1×10^5
DA-CB8^a	4.2×10^4
GA-CB7^b	3.2×10^6
GA-CB8^c	1.4×10^{10}
1o-CB7^d	1.0×10^3
1o-CB8^e	6.5×10^6
1c-CB7^d	1.0×10^3
1c-CB8^e	2.2×10^{10}

^a Taken from ref. 16. ^b Taken from ref. 52. ^c Taken from ref. 49.

^d Measured in this work by ^1H NMR titration (see ESI). ^e Taken from ref. 51.



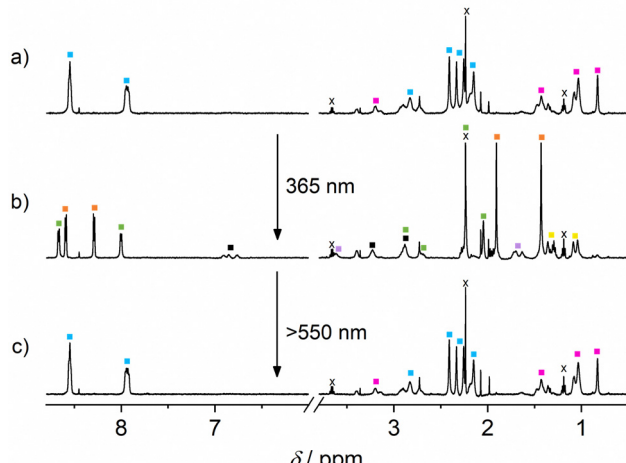


Fig. 3 The ^1H NMR spectra (500 MHz, in D_2O at $\text{pD} 5.4$) of (a) the initial five-component mixture, (b) after irradiation (15 min) with 365 nm light ($\mathbf{1o} \rightarrow \mathbf{1c}$), and (c) after back-isomerization (20 min) with light >550 nm ($\mathbf{1c} \rightarrow \mathbf{1o}$). $[\mathbf{1}] = 300 \mu\text{M}$; $[\mathbf{GA}] = [\mathbf{DA}] = [\mathbf{CB7}] = [\mathbf{CB8}] = 200 \mu\text{M}$. Colour codes: ■: $\mathbf{1o}$, ■: $\mathbf{1c}$, ■: $\mathbf{GA}\text{-CB8}$, ■: $\mathbf{1c}\text{-CB8}$, ■: $\mathbf{GA}\text{-CB7}$, ■: \mathbf{DA} , and ■: \mathbf{GA} . x denotes solvent impurities (traces of diethylether, acetone).

of released **DA** and the total amount of **DA** (released by adding 500 μM 3-aminoadamant-1-ol)¹⁹ it can be estimated that *ca.* 50% of **DA** is released in the light-induced cascade.⁵³ On shining visible light (>550 nm) on the $\mathbf{1c}$ form, $\mathbf{1o}$ is formed back quantitatively ($\Phi_{\mathbf{1c} \rightarrow \mathbf{1o}} = 0.001$)⁵¹ and consequently the initial situation is restored (see Fig. 3c). The ^1H NMR spectra before 365 nm irradiation and after irradiation with visible light are practically indistinguishable (Fig. 3a and c).

The simulation of the distribution of the constituents of the cascade before and after irradiation with UV light provides further insights into the correct function of the cascade; see

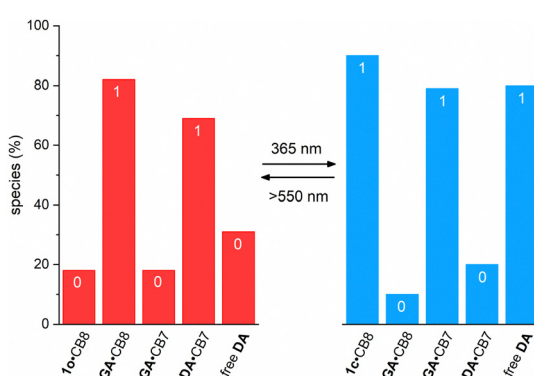


Fig. 4 Predicted distribution of the different host–guest complexes and the free **DA** in the five-component mixture, containing either $\mathbf{1o}$ (left) or $\mathbf{1c}$ (right). The percentage values of the complexes refer to percentage of the corresponding host concentration (CB7 or CB8), while the percentage value of free **DA** refers to the fraction of the total **DA**. All values are comparable among each other due to the fact that equimolar concentrations were used for **GA**, **DA**, CB7, and CB8 (200 μM). If low percentage values are assigned a binary 0 and high values a binary 1, then the initial situation (left) corresponds to the pattern 01010. However, the light-induced changes (right) lead to the inverted binary pattern (10101), which is in agreement with the intended cascade.

Fig. 4. This prediction is based on the coupled thermodynamic equilibria of the involved host–guest complexes (see ESI†). Before irradiation about 82% of all CB8 are occupied by **GA** and 69% of all CB7 capsules have **DA** as a guest. On 365 nm light irradiation, the ring-closed DTE $\mathbf{1c}$ is formed and now about 90% of all CB8 have this one as a guest. Consequently, the released **GA** competes with **DA** for the CB7 cavity and 79% of all CB7 have the former as a guest, while only 20% retain **DA**. This means that about 80% of all **DA** is non-bound after irradiation, compared to 31% before irradiation. This corresponds to about 50% light-induced release of **DA**, being in excellent agreement with the experiment (see above).

It should be stressed that the mediator function of **GA** is strictly necessary to release **DA** from CB7, because neither form of $\mathbf{1}$, open or closed, could displace **DA** directly from CB7. This is because both $\mathbf{1o}$ and $\mathbf{1c}$ have binding constants with CB7 that are two orders of magnitude lower than that of **DA**. The impossibility to release **DA** by means of competitive displacement with $\mathbf{1c}$ was demonstrated by a corresponding ^1H NMR experiment (see ESI†). All observed signals in the three-component mixture ($[\mathbf{1}] = 300 \mu\text{M}$; $[\mathbf{DA}] = [\mathbf{CB7}] = 200 \mu\text{M}$) correspond perfectly to those of non-bonded DTE (either $\mathbf{1o}$ or $\mathbf{1c}$). In addition, no NMR signals of free **DA** were observed after the light-induced conversion of $\mathbf{1o}$ into $\mathbf{1c}$.

In summary, we report a light-triggered supramolecular cascade that transduces a photonic signal into the release of dopamine. The cascade builds on the principles of thermodynamic self-sorting. On conversion of a DTE phototrigger a different equilibrium situation is created, which translates into downstream cascading and the final release of the neurotransmitter. These characteristics are also found in the vision process, mimicked by the herein described system. This may be of interest for (supra)molecular information processing,^{54–57} where stimuli-dependent concentration patterns may be of importance,^{49,58} or as light-dependent actuators.

This work was supported by the Spanish Ministerio de Ciencia e Innovación (grant PID2020-119992GB-I00 for U.P.), the Consejería de Economía, Conocimiento, Empresas y Universidad/Junta de Andalucía (grant P18-FR-4080 for U.P.), the Portuguese Fundação para a Ciência e a Tecnologia – FCT/MCTES (grant CEECIND/00466/2017 for N.B.), and by LAQV-REQUIMTE (through UIDB/50006/2020 and UIDP/50006/2020).

Conflicts of interest

There are no conflicts to declare.

References

- 1 R. S. H. Liu and A. E. Asato, *Proc. Natl. Acad. Sci. U. S. A.*, 1985, **82**, 259–263.
- 2 Y. Shichida and T. Matsuyama, *Philos. Trans. R. Soc., B*, 2009, **364**, 2881–2895.
- 3 T. Munteanu, K. J. Noronha, A. C. Leung, S. Pan, J. A. Lucas and T. M. Schmidt, *eLife*, 2018, **7**, e39866.
- 4 D.-H. Qu, Q.-C. Wang, Q.-W. Zhang, X. Ma and H. Tian, *Chem. Rev.*, 2015, **115**, 7543–7588.
- 5 A. Díaz-Moscoso and P. Ballester, *Chem. Commun.*, 2017, **53**, 4635–4652.

6 D. Ray, J. T. Foy, R. P. Hughes and I. Aprahamian, *Nat. Chem.*, 2012, **4**, 757–762.

7 S. Ma, M. M. J. Smulders, Y. R. Hristova, J. K. Clegg, T. K. Ronson, S. Zarra and J. R. Nitschke, *J. Am. Chem. Soc.*, 2013, **135**, 5678–5684.

8 A. G. Salles Jr., S. Zarra, R. M. Turner and J. R. Nitschke, *J. Am. Chem. Soc.*, 2013, **135**, 19143–19146.

9 M. Schmittel, *Chem. Commun.*, 2015, **51**, 14956–14968.

10 G. Ashkenasy, T. M. Hermans, S. Otto and A. F. Taylor, *Chem. Soc. Rev.*, 2017, **46**, 2543–2554.

11 M. J. Langton, F. Keymeulen, M. Ciaccia, N. H. Williams and C. A. Hunter, *Nat. Chem.*, 2017, **9**, 426–430.

12 A. Llopis-Lorente, P. Díez, A. Sánchez, M. D. Marcos, F. Sancenón, P. Martínez-Ruiz, R. Villalonga and R. Martínez-Máñez, *Nat. Commun.*, 2017, **8**, 15511–15517.

13 B. S. Pilgrim, D. A. Roberts, T. G. Lohr, T. K. Ronson and J. R. Nitschke, *Nat. Chem.*, 2017, **9**, 1276–1281.

14 J. S. Park, J. Park, Y. J. Yang, T. T. Tran, I. S. Kim and J. L. Sessler, *J. Am. Chem. Soc.*, 2018, **140**, 7598–7604.

15 Y.-C. Liu, W. M. Nau and A. Hennig, *Chem. Commun.*, 2019, **55**, 14123–14126.

16 P. Remón, D. González, M. A. Romero, N. Basílio and U. Pischel, *Chem. Commun.*, 2020, **56**, 3737–3740.

17 S. Liu, C. Ruspic, P. Mukhopadhyay, S. Chakrabarti, P. Y. Zavalij and L. Isaacs, *J. Am. Chem. Soc.*, 2005, **127**, 15959–15967.

18 K. I. Assaf and W. M. Nau, *Chem. Soc. Rev.*, 2015, **44**, 394–418.

19 S. J. Barrow, S. Kasera, M. J. Rowland, J. del Barrio and O. A. Scherman, *Chem. Rev.*, 2015, **115**, 12320–12406.

20 L. P. Cao, M. Šekutor, P. Y. Zavalij, K. Mlinarić-Majerski, R. Glaser and L. Isaacs, *Angew. Chem., Int. Ed.*, 2014, **53**, 988–993.

21 J. M. Chinai, A. B. Taylor, L. M. Ryno, N. D. Hargreaves, C. A. Morris, P. J. Hart and A. R. Urbach, *J. Am. Chem. Soc.*, 2011, **133**, 8810–8813.

22 D.-W. Lee, K. M. Park, M. Banerjee, S. H. Ha, T. Lee, K. Suh, S. Paul, H. Jung, J. Kim, N. Selvapalam, S. H. Ryu and K. Kim, *Nat. Chem.*, 2011, **3**, 154–159.

23 I. Ghosh and W. M. Nau, *Adv. Drug Delivery Rev.*, 2012, **64**, 764–783.

24 Y. Ahn, Y. Jang, N. Selvapalam, G. Yun and K. Kim, *Angew. Chem., Int. Ed.*, 2013, **52**, 3140–3144.

25 F. Biedermann and W. M. Nau, *Angew. Chem., Int. Ed.*, 2014, **53**, 5694–5699.

26 S. Zhang, K. I. Assaf, C. Huang, A. Hennig and W. M. Nau, *Chem. Commun.*, 2019, **55**, 671–674.

27 C. M. Hu, T. Jochmann, P. Chakraborty, M. Neumaier, P. A. Levkin, M. M. Kappes and F. Biedermann, *J. Am. Chem. Soc.*, 2022, **144**, 13084–13095.

28 A. Prabodh, S. Sinn and F. Biedermann, *Chem. Commun.*, 2022, **58**, 13947–13950.

29 M. L. Pellizzaro, K. A. Houton and A. J. Wilson, *Chem. Sci.*, 2013, **4**, 1825–1829.

30 M. Han, R. Michel, B. He, Y.-S. Chen, D. Stalke, M. John and G. H. Clever, *Angew. Chem., Int. Ed.*, 2013, **52**, 1319–1323.

31 D. V. Berdnikova, T. M. Aliyu, T. Paululat, Y. V. Fedorov, O. A. Fedorova and H. Ihmels, *Chem. Commun.*, 2015, **51**, 4906–4909.

32 G. Yu, W. Yu, Z. Mao, C. Gao and F. Huang, *Small*, 2015, **11**, 919–925.

33 L. Stricker, E.-C. Fritz, M. Peterlechner, N. L. Doltsinis and B. J. Ravoo, *J. Am. Chem. Soc.*, 2016, **138**, 4547–4554.

34 S. T. J. Ryan, J. del Barrio, R. Suardiaz, D. F. Ryan, E. Rosta and O. A. Scherman, *Angew. Chem., Int. Ed.*, 2016, **55**, 16096–16100.

35 A. Tron, I. Pianet, A. Martinez-Cuezva, J. H. R. Tucker, L. Pisciottani, M. Alajarín, J. Berna and N. D. McClenaghan, *Org. Lett.*, 2017, **19**, 154–157.

36 X. D. Chi, W. L. Cen, J. A. Queenan, L. L. Long, V. M. Lynch, N. M. Khashab and J. L. Sessler, *J. Am. Chem. Soc.*, 2019, **141**, 6468–6472.

37 R. J. Li, J. J. Holstein, W. G. Hiller, J. Andréasson and G. H. Clever, *J. Am. Chem. Soc.*, 2019, **141**, 2097–2103.

38 A. Ducrot, A. Tron, R. Bofinger, I. Sanz Beguer, J.-L. Pozzo and N. D. McClenaghan, *Beilstein J. Org. Chem.*, 2019, **15**, 2801–2811.

39 M. Canton, A. B. Grommet, L. Pesce, J. Germen, S. Li, Y. Diskin-Posner, A. Credi, G. M. Pavan, J. Andréasson and R. Klajn, *J. Am. Chem. Soc.*, 2020, **142**, 14557–14565.

40 F. Tian, D. Jiao, F. Biedermann and O. A. Scherman, *Nat. Commun.*, 2012, **3**, 1207.

41 N. Basílio and U. Pischel, *Chem. – Eur. J.*, 2016, **22**, 15208–15211.

42 J. del Barrio, S. T. J. Ryan, P. G. Jambrina, E. Rosta and O. A. Scherman, *J. Am. Chem. Soc.*, 2016, **138**, 5745–5748.

43 M. A. Romero, R. J. Fernandes, A. J. Moro, N. Basílio and U. Pischel, *Chem. Commun.*, 2018, **54**, 13335–13338.

44 M. Irie, T. Fukaminato, K. Matsuda and S. Kobatake, *Chem. Rev.*, 2014, **114**, 12174–12277.

45 M. Herder, B. M. Schmidt, L. Grubert, M. Pätz, J. Schwarz and S. Hecht, *J. Am. Chem. Soc.*, 2015, **137**, 2738–2747.

46 J. Zhang and H. Tian, *Adv. Opt. Mater.*, 2018, **6**, 1701278.

47 G. Liu, Y.-M. Zhang, C. Wang and Y. Liu, *Chem. – Eur. J.*, 2017, **23**, 14425–14429.

48 P. Ferreira, B. Ventura, A. Barbieri, J. P. Da Silva, C. A. T. Laia, A. J. Parola and N. Basílio, *Chem. – Eur. J.*, 2019, **25**, 3477–3482.

49 P. Remón, D. González, S. M. Li, N. Basílio, J. Andréasson and U. Pischel, *Chem. Commun.*, 2019, **55**, 4335–4338.

50 D. Kim, A. Aktalay, N. Jensen, K. Uno, M. L. Bossi, V. N. Belov and S. W. Hell, *J. Am. Chem. Soc.*, 2022, **144**, 14235–14247.

51 P. Máximo, M. Colaço, S. R. Pauleta, P. J. Costa, U. Pischel, A. J. Parola and N. Basílio, *Org. Chem. Front.*, 2022, **9**, 4238–4249.

52 M. A. Romero, N. Basílio, A. J. Moro, M. Domingues, J. A. González-Delgado, J. F. Arteaga and U. Pischel, *Chem. – Eur. J.*, 2017, **23**, 13105–13111.

53 It should be noted that the ^1H NMR signals of the released dopamine are rather broad. Therefore, the error of the stated release percentage is relatively large and conservatively estimated as *ca.* 15%.

54 A. P. de Silva and S. Uchiyama, *Nat. Nanotechnol.*, 2007, **2**, 399–410.

55 J. Kärnbratt, M. Hammarskjöld, S. Li, H. L. Anderson, B. Albinsson and J. Andréasson, *Angew. Chem., Int. Ed.*, 2010, **49**, 1854–1857.

56 J. Andréasson and U. Pischel, *Chem. Soc. Rev.*, 2015, **44**, 1053–1069.

57 S. Erbas-Cakmak, S. Kolemen, A. C. Sedgwick, T. Gunnlaugsson, T. D. James, J. Yoon and E. U. Akkaya, *Chem. Soc. Rev.*, 2018, **47**, 2228–2248.

58 A. Ghosh, I. Paul and M. Schmittel, *J. Am. Chem. Soc.*, 2019, **141**, 18954–18957.

